**Zeitschrift:** Helvetica Physica Acta

**Band:** 58 (1985)

**Heft:** 2-3

**Artikel:** Resonant Raman scattering in ZrS\_3 and ZrSe\_3

Autor: Kurita, S. / Okada, Y. / Tanaka, M.

**DOI:** https://doi.org/10.5169/seals-115601

### Nutzungsbedingungen

Die ETH-Bibliothek ist die Anbieterin der digitalisierten Zeitschriften auf E-Periodica. Sie besitzt keine Urheberrechte an den Zeitschriften und ist nicht verantwortlich für deren Inhalte. Die Rechte liegen in der Regel bei den Herausgebern beziehungsweise den externen Rechteinhabern. Das Veröffentlichen von Bildern in Print- und Online-Publikationen sowie auf Social Media-Kanälen oder Webseiten ist nur mit vorheriger Genehmigung der Rechteinhaber erlaubt. Mehr erfahren

### **Conditions d'utilisation**

L'ETH Library est le fournisseur des revues numérisées. Elle ne détient aucun droit d'auteur sur les revues et n'est pas responsable de leur contenu. En règle générale, les droits sont détenus par les éditeurs ou les détenteurs de droits externes. La reproduction d'images dans des publications imprimées ou en ligne ainsi que sur des canaux de médias sociaux ou des sites web n'est autorisée qu'avec l'accord préalable des détenteurs des droits. En savoir plus

### Terms of use

The ETH Library is the provider of the digitised journals. It does not own any copyrights to the journals and is not responsible for their content. The rights usually lie with the publishers or the external rights holders. Publishing images in print and online publications, as well as on social media channels or websites, is only permitted with the prior consent of the rights holders. Find out more

**Download PDF:** 29.11.2025

ETH-Bibliothek Zürich, E-Periodica, https://www.e-periodica.ch

# Resonant Raman scattering in ZrS<sub>3</sub> and ZrSe<sub>3</sub>

By S. Kurita, Y. Okada and M. Tanaka, Laboratory of Applied Physics, Faculty of Engineering, Yokohama National University, Hodogaya, Yokohama 240, Japan F. Lévy, Institut de Physique Appliquée, Ecole Polytechnique Fédérale, 1015 Lausanne, Switzerland

(2. X. 1984)

In honor of Emanuel Mooser's 60th birthday

Abstract. The resonant Raman scattering by several  $A_g$  phonons has been measured at the region of the exciton band for  $ZrS_3$  and  $ZrSe_3$ . The excitation spectra and the polarization dependence of  $ZrS_3$  are quite similar to those of  $ZrSe_3$  at the resonant region. It is proposed, by comparing with the Raman spectra out of the exciton region, that the electronic states related to the Raman scattering processes are composed of the antibonding p orbitals of chalcogen molecules at the exciton band region, but the transition metal d orbitals at the high energy region. The incident photon energy dependence of the Raman cross section at the exciton absorption band is well explained with a single oscillator of the 1s exciton.

### 1. Introduction

Transition metal trichalcogenides  $(MX_3)$  have significant one dimensional anisotropic character in its crystal structure [1]. The transition metal atoms lie at the center of distorted trigonal prisms which share trigonal faces forming isolated chains. The chains run parallel to the b crystallographic axis and are displaced from neighboring columns by one half the unit cell along the b axis. In a chain, one of chalcogen-chalcogen (X-X) pairs which forms one side of a prism has the distance shorter than any other pairs. Because of this crystal structure, it is suggested that some of chalcogen atoms are bound together as like  $(X_2)^{2-}$  and act as single ligands. This suggestion has been confirmed by the analysis of photoemission spectrum [2, 3].

Optical absorption spectra indicate indirect band gap for both  $ZrS_3$  and  $ZrSe_3$  [4]. The electronic states related to this indirect gap are shown to have rather three dimensional properties. The exciton due to direct transition has been observed for both materials on the  $E \parallel b$  configuration where the electric field of light E is parallel to the b axis. For the  $E \perp b$  configuration, a weak absorption band has been observed on  $ZrS_3$  at the lower energy of 0.1 eV than the direct exciton, but there is no significant absorption structure on  $ZrSe_3$ . The short distance of the X-X pair forces the energy of their antibonding states to be higher than the energy of the single chalcogen p states, so that the conduction and valence bands are composed of the antibonding p orbitals of the chalcogen molecules mainly. The strong absorption band of the exciton at the absorption edge is due to the transition between the antibonding p orbitals. The discrepancy

of the absorption spectra on  $E \perp b$ , however, is not explained only by the electronic states which are constructed by these antibonding p orbitals. This shows that one should take into account the metal d orbitals for the conduction and valence bands, but one has little information how much the metal d orbitals are mixed and have effect on the absorption and Raman spectra.

There are extensive studies of the lattice dynamics on ZrS<sub>3</sub> and ZrSe<sub>3</sub> [5–8]. Almost all long-wavelength phonons are identified with the aid of the measurements of Raman and infrared spectra and of theoretical calculation [8]. As seen later in Fig. 1, however, the Raman spectra of ZrS<sub>3</sub> and ZrSe<sub>3</sub> are quite different. The polarization dependence of Raman intensity of ZrS<sub>3</sub> is completely contrary to that of ZrSe<sub>3</sub> for the same phonons.

From the results of resonant Raman scattering measurements this report shows that this discrepancy in the Raman spectra is due to the difference between the electronic states related to the Raman scattering processes. It is also proposed that the electronic states at the absorption edge are composed of the antibonding p orbitals of the chalcogen molecules mainly, but in the high energy region the metal d orbitals are mixed. At the last part of this report, it is shown that the

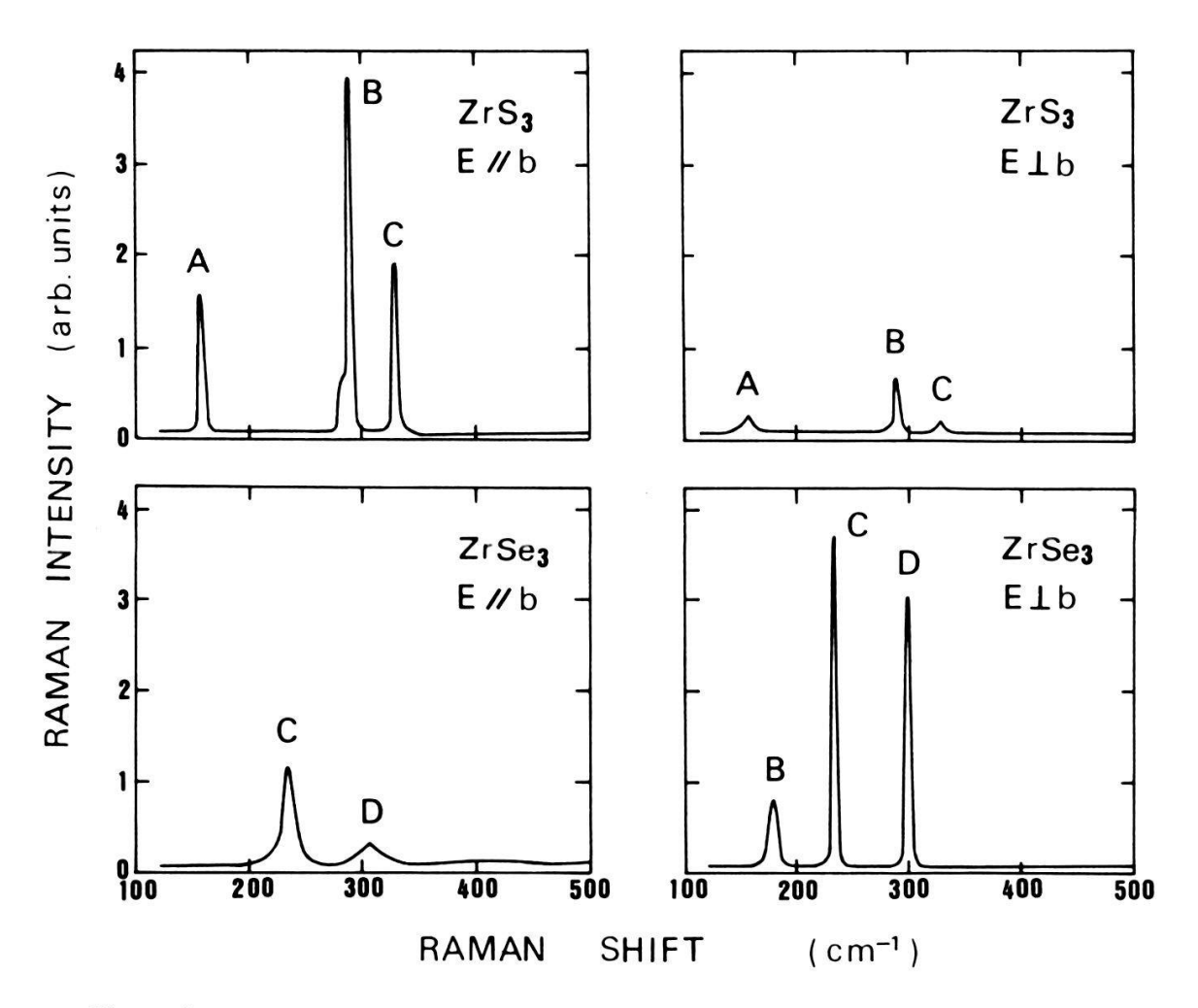


Figure 1 Raman spectra of  $ZrS_3$  and  $ZrSe_3$  for the excitation by 514.5 nm line of Ar-ion laser at room temperature.  $E \parallel b$  and  $E \perp b$  denote  $E_i \parallel E_s \parallel b$  and  $E_i \parallel E_s \perp b$ , respectively where the b axis is taken along the chain. A, B etc. are used to distinguish the vibrational modes in the  $A_g$  phonons.

incident photon energy dependence of the Raman cross section at the absorption edge is well explained with a single oscillator model of the 1s exciton [9].

# 2. Experiments

Vol. 58, 1985

All measurements were done using the as-grown single crystals (not cleaved) whose surfaces were parallel to the (a, b) plane. The light was always at normal incidence of the crystal surface. Because of the large dichroism of the crystal, the optical system had to be carefully aligned. The polarization direction of the light with respect to the crystal axis was determined by measuring the reflectivity as a function of the polarizer angle in the spectral region of the direct band gap where the effect of dichroism is largest. The samples were immersed in a superfluid helium bath for the low temperature measurements.

Raman scattering experiments were carried out in the geometry of back scattering. The light from the Kr- and Ar-ion lasers and the dye laser which was excited by Kr, Ar and  $N_2$  lasers was used. Spectra were obtained with incident power of less than 20 mW at room temperature (50 mW at 2 K) to prevent the sample from overheating and decomposing. The scattered light was spectrally analyzed with a 1 m double monochromator and detected with a standard photon counting technique for the cw laser excitation and with a boxcar integrator method for the pulse laser excitation.

## 3. Experimental results and discussion

Figure 1 shows the Raman spectra at room temperature for the excitation by the 514.5 nm (2.41 eV) line of the Ar-ion laser.  $E \parallel b$  and  $E \perp b$  in the figure denote the polarization configuration of  $Y(ZZ)\bar{Y}$  and  $Y(XX)\bar{Y}$ , respectively, where Z is taken along the chain axis and X along the a axis. The Raman active modes are  $A_g$  and  $B_g$  in terms of the selection rule formulated by Loudon [9]. All the phonons observed here are identified to be the  $A_g$  phonons according to the analysis of Grisel et al. [8]. The notation of A, B, etc. in the figure is used to distinguish the vibrational modes, that is, the phonon B of ZrS<sub>3</sub>, for example, has the same vibrational property as the phonon B of ZrSe<sub>3</sub>.

If one takes notice of B and C phonons, the Raman intensity on  $E \parallel b$  is much larger than that on  $E \perp b$  for  $ZrS_3$ . On the other hand, the intensity on  $E \parallel b$  for  $ZrSe_3$  is smaller than that on  $E \perp b$ , so that the polarization dependence of the Raman intensity of  $ZrS_3$  is contrary to that of  $ZrSe_3$ . As  $ZrS_3$  and  $ZrSe_3$  have the same crystal structure with a highly anisotropic system and the same electronic configuration of valence, one would expect the same polarization dependence of the Raman spectra for the same phonon. For understanding the observed difference on the polarization dependence, one should notice that the exciting photon energy (2.41 eV) is much higher than the direct absorption edge of  $ZrSe_3$  (1.8 eV), but just below that of  $ZrS_3$  (2.5 eV) [4]. This suggests that the electronic states concerned with the Raman scattering processes for  $ZrS_3$  are different from those for  $ZrSe_3$ .

Jellinek et al. [2] have proposed that the absorption bands at the energy region of the absorption edge are due to the transition between the antibonding p

orbitals of chalcogen molecule  $(X_2)^{2-}$ . A recent band calculation of  $ZrSe_3$  [10] indicates that the valence band maximum occurs at the  $\Gamma$  point and that the conduction band minimum as well as the direct gap occurs at the A points in the Brillouin zone, and also that these valence and conduction bands are composed of mainly the p orbitals of chalcogen. A recent photoemission experiment [11] on the mixed crystals of  $Zr_{1-x}Ti_xS_3$ , however, shows that in the high energy region the s and d orbitals of the transition metal are strongly mixed with the p orbitals of the chalcogen.

The difference between the electronic states at the absorption edge and those at higher energy explains why the Raman spectra of  $ZrS_3$  are different from those of  $ZrSe_3$  for the same lattice vibrational modes; the electronic states which are most effective to the Raman scattering processes are the antibonding p orbitals of  $(X_2)^{2-}$  for  $ZrS_3$ , but mainly metal d orbitals for  $ZrSe_3$ . This difference in the related electronic states affects the polarization dependence. This interpretation for the discrepancy of the Raman spectra will be confirmed if one has the same Raman spectra when the excitation energy is tuned to the exciton absorption band at the absorption edge which is settled to be due to a transition between the antibonding p orbitals of the chalcogen molecules for both materials [2, 4, 10].

Figure 2 shows the Raman spectra of  $Y(ZZ)\bar{Y}$   $(E\parallel b)$  configuration with the incident photon energy of 2.602 eV for  $ZrS_3$  and of 1.830 eV for  $ZrSe_3$  where the photon energy is at each exciton absorption band. The Raman intensity of the polarization  $Y(XX)\bar{Y}$   $(E\perp b)$  at these photon energies is smaller of one order than that of  $Y(ZZ)\bar{Y}$   $(E\parallel b)$  for both materials. There is no discrepancy in the polarization dependence of the Raman intensity, showing that the electronic states forming the exciton at the band edge are the same for both  $ZrS_3$  and  $ZrSe_3$ .

The Raman cross section in the case of the back scattering at normal incidence from a semi-infinite crystal can be calculated if one knows the absorp-

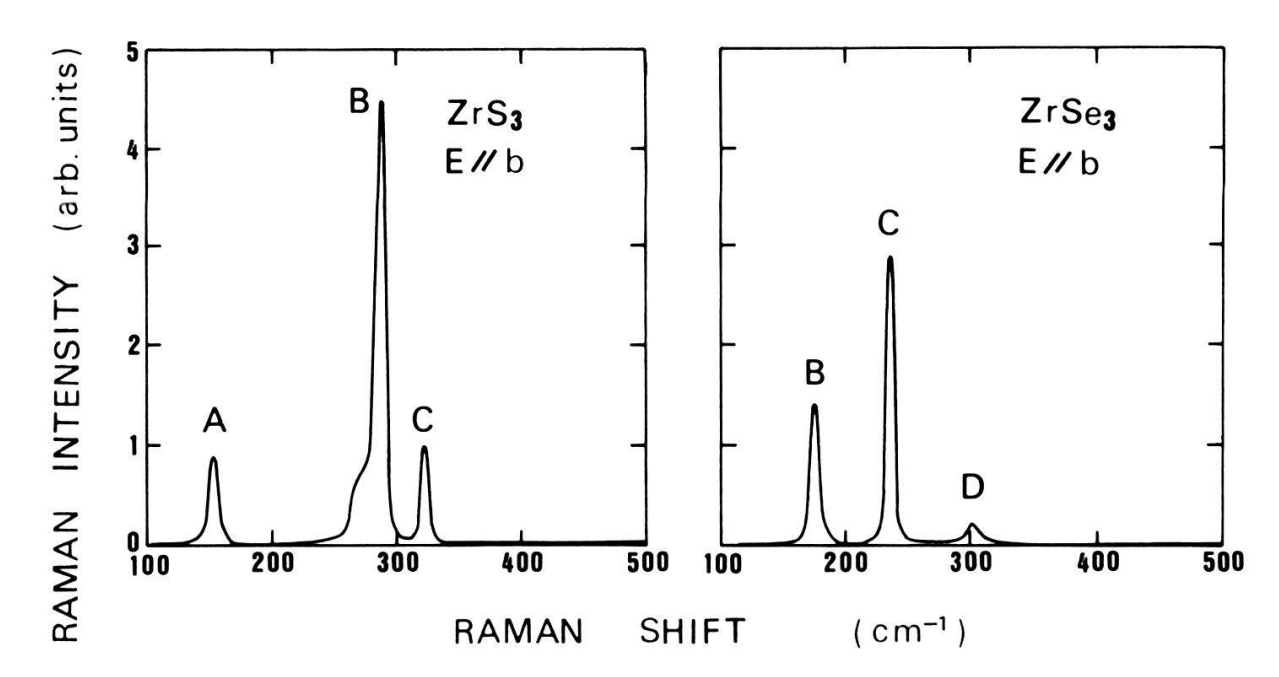


Figure 2 Raman spectra on the  $E \parallel b$  configuration at 2 K. The incident photon energies are 2.602 eV for  $ZrS_3$  and 1.830 eV for  $ZrSe_3$  which are the peak energies of the exciton absorption bands. The Raman intensity on  $E \perp b$  is smaller of one order than that on  $E \parallel b$  for both  $ZrSe_3$  and  $ZrSe_3$ .

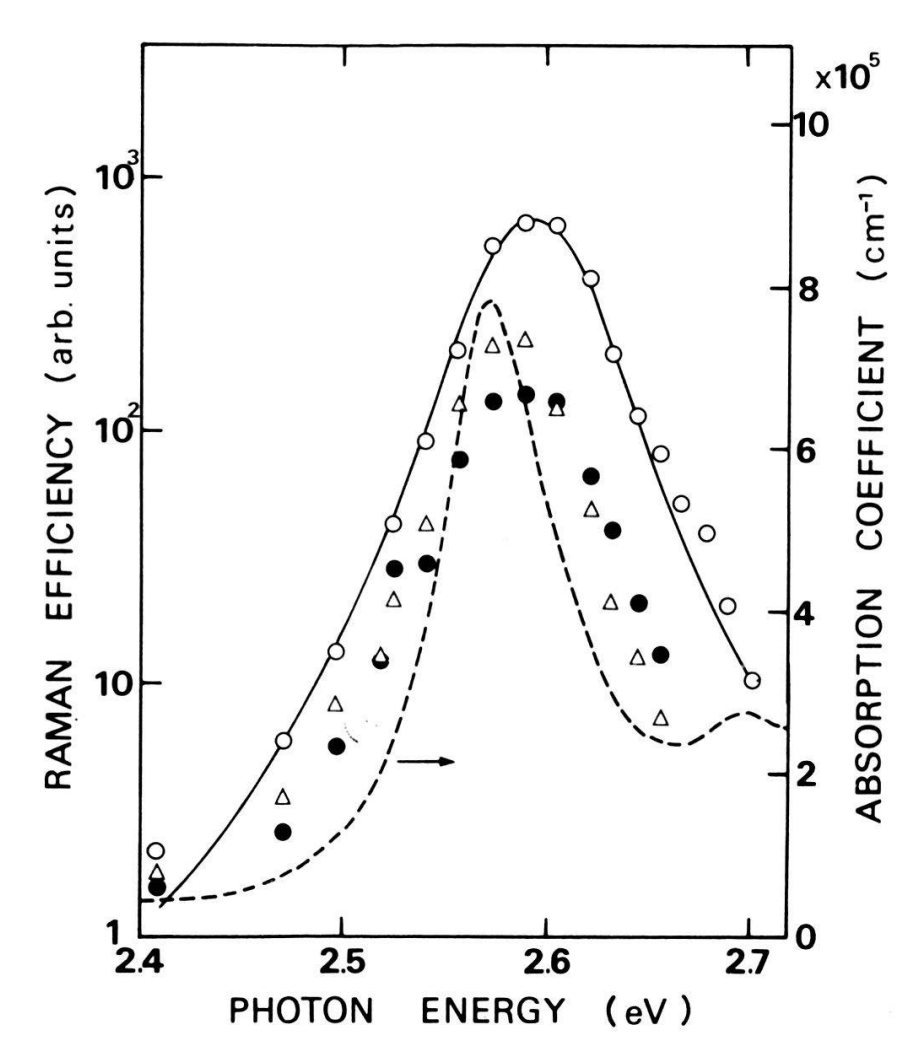


Figure 3
Raman efficiency of  $ZrS_3$  at the exciton absorption band as a function of the incident photon energy on the  $E \parallel b$  configuration for the several  $A_g$  phonons which frequencies are 19.0 meV ( $\triangle$ ), 35.7 meV ( $\bigcirc$ ) and 40.4 meV ( $\bigcirc$ ). The solid curve is the calculated Raman cross section for the phonon of 35.7 meV ( $\bigcirc$ ) where the exciton energy  $\hbar\omega_{\alpha}$  and the damping energy  $\hbar\Gamma$  is taken as 2.575 eV and 35 meV, respectively. The absorption spectrum is shown by the broken line for comparison.

tion coefficients and the reflectivities at the incident photon energy and at the scattered photon energy [9]. The reflectivity and the absorption coefficient have been obtained by measuring the reflectivity and by performing the Kramers-Kronig analysis [12]. Figures 3 and 4 show the excitation spectra of the Raman scattering for several  $A_{\rm g}$  phonons at 2 K for ZrS<sub>3</sub> and ZrSe<sub>3</sub>, respectively, where the Raman intensity has been corrected for absorption as well as reflectance. The change in the  $\omega^4$  factor of the scattering law is negligibly small in the narrow spectral range of the measurement. In the figures the absorption spectra are also shown by the broken lines for comparison.

The excitation spectra at the absorption edge and the dependence of the Raman spectra on the light polarization are quite similar for both materials. This experimental result shows that our interpretation is correct: The electronic states at the band edge are constructed by the same orbitals, that is, antibonding p orbitals of chalcogen molecules  $(X_2)^{2-}$ , but in the high energy region the metal d orbitals take main parts of the electronic states on the Raman scattering processes.

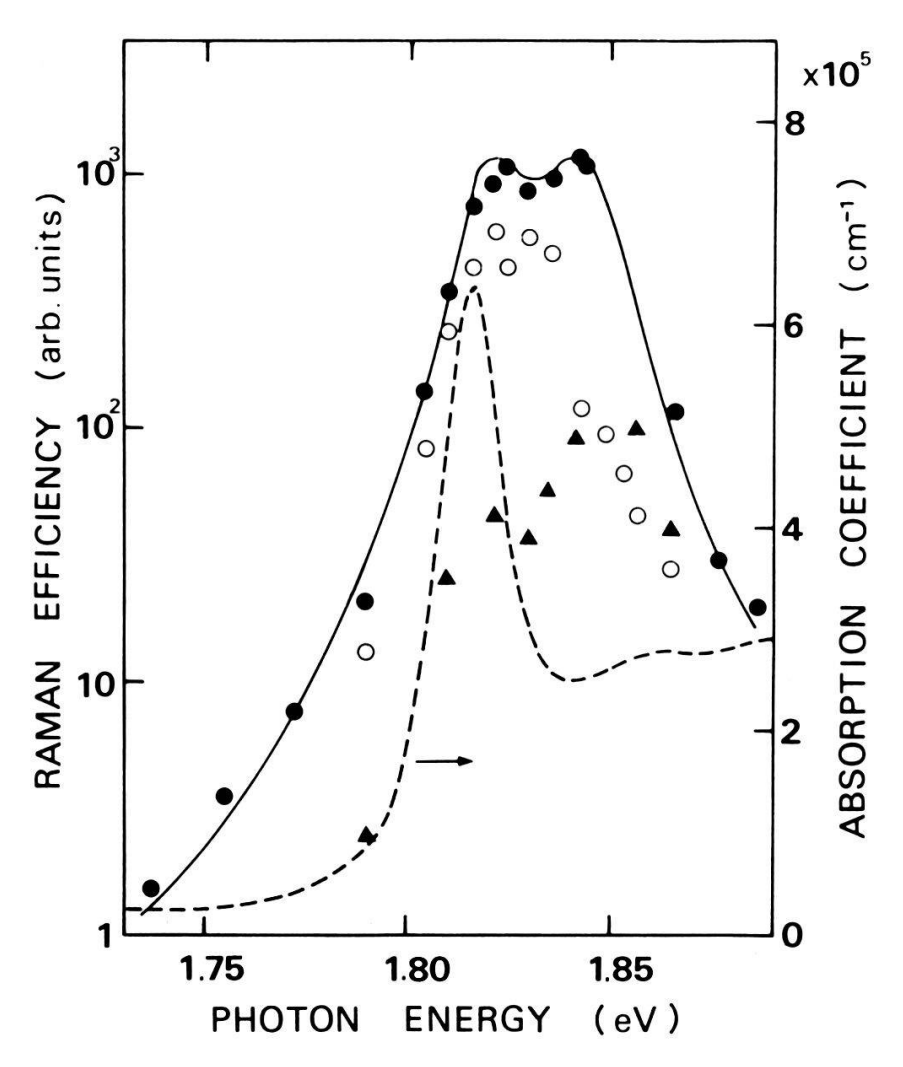


Figure 4
Raman efficiency of  $ZrSe_3$  at the exciton absorption band as a function of the incident photon energy on the  $E \parallel b$  configuration for the several  $A_g$  phonons which frequencies are 22.3 meV ( $\bigcirc$ ), 29.3 meV ( $\bigcirc$ ) and 37.8 meV ( $\triangle$ ). The solid curve is the calculated Raman cross section for the phonon of 29.3 meV ( $\bigcirc$ ) where the exciton energy  $\hbar\omega_{\alpha}$  and the damping energy  $\hbar\Gamma$  is taken as 1.820 eV and 10 meV, respectively. The absorption spectrum is shown by the broken line for comparison.

The Raman cross section for the first order process is approximately written as [9]

$$\sigma \propto \sum_{\alpha,\beta} \left| \frac{P_{0\beta} \Xi_{\beta\alpha} P_{\alpha0}}{(\omega_e + i \Gamma - \omega_i)(\omega_\alpha + i \Gamma - \omega_i)} \right|^2 \delta(\omega_i - \Omega - \omega_s)$$

where  $\omega_i$ ,  $\omega_s$  and  $\Omega$  are the frequency of the incident light, the scattered light and the associated phonon, respectively;  $P_{\alpha 0}$  is the momentum matrix element which subscripts, 0 and  $\alpha$ , refer to the electronic ground state and the intermediate one, respectively.  $\Xi_{\beta\alpha}$  is the matrix element of the electron (exciton) phonon interaction and  $\Gamma$  the phenomenological damping constant.

The Raman excitation spectra are analyzed with a single oscillator model for two reasons: Only a large absorption band due to 1s exciton formation is observed at the absorption edge for both materials and, if the incident photon energy is close to the 1s exciton energy, the cross sections are little influenced by the resonance Raman scattering process where the higher exciton and the continuum states are intermediate states. Then, one can estimate the Raman efficiency for each phonon, with the adjustable parameter  $\Gamma$ , under the assumption that the matrix elements  $P_{0\alpha}$  and  $\Xi_{\beta\alpha}$  are independent of  $\omega_i$ . The most reliable calculated curves for a phonon are shown with solid lines in Figs. 3 and 4 using following values;  $\hbar\omega_{\alpha}=2.575\,\mathrm{eV},~\hbar\Omega=35.7\,\mathrm{meV},~\hbar\Gamma=35\,\mathrm{meV}$  for  $\mathrm{ZrS_3}$  and  $\hbar\omega_{\alpha}=1.818\,\mathrm{eV},~\hbar\Omega=29.3\,\mathrm{meV},~\hbar\Gamma=10\,\mathrm{meV}$  for  $\mathrm{ZrSe_3}$ . The calculated curves give a very good agreement with the experimental points. In  $\mathrm{ZrSe_3}$ , a small damping value compared to the phonon energy causes the excitation spectrum to have two maximums, that is, resonant parts of the incoming light and of the outgoing light. In  $\mathrm{ZrS_3}$ , there is no splitting on the excitation spectrum because of the large damping effect. The large damping effect also causes the peak of the excitation spectrum to locate at the middle of  $\hbar\omega_{\alpha}$  and  $\hbar\omega_{\alpha}+\hbar\Omega$ .

### Conclusion

It is shown that the polarization dependence of the Raman spectra of  $ZrS_3$  is contrary to that of  $ZrSe_3$  if the 514.5 nm line of the Ar-ion laser is used as excitation. The Raman cross section for both materials, however, is shown to be quite similar at the energy region of the exciton absorption band which is settled to be due to a transition between the antibonding p orbitals of the chalcogen molecules. These experimental results suggest that the electronic states at the pand edge are composed of the antibonding p orbitals, but the d orbitals of the transition metal are mixed at the high energy region. The incident photon energy dependence of the Raman cross section at the absorption edge is well explained with a single oscillator model of the 1s exciton.

### Acknowledgements

The present work was started during the stay of one of the authors (S.K.) at the institute of Prof. E. Mooser (EPFL). The authors wish to express their thanks to him for his continuous encouragements throughout this work. The authors would also like to thank Prof. Y. Nishina (Tohoku University in Japan) and the members of his laboratory for very fruitful discussions and for using their facilities with which a part of the resonant Raman scattering measurements were done.

#### REFERENCES

- [1] W. KRONERT and V. PLIETH, Z. Anorg. Allg. Chem. 32, 207 (1965).
- [2] F. JELLINEK, R. A. POLLAK and M. W. SHAFER, Mat. Res. Bull., 9, 845 (1974).
- [3] G. MARGARITONDO, A. D. KATNANI, N. G. STOFFEL And F. LÉVY, J. Electron Spectrosc. Relat. Phenom., 20, 69 (1980).
- [4] S. Kurita, J. L. Staehli, M. Guzzi and F. Lévy, Physica, 105B, 169 (1981).
- [5] S. JANDL, C. DEVILLE CAVELLIN and J. Y. HARBEC, Solid State Commun., 31, 351 (1979).
- [6] T. ADACHI, T. GOTO and Y. NISHINA, J. Lumin., 21, 169 (1980).
- [7] T. J. WIETING, A. GRISEL, F. LÉVY and PH. SCHMID, Proc. Int. Conf. Quasi-One-Dimensional Conductors. Dubrovnik 1978, Lecture Notes in Physics 95 (Springer-Verlag, Berlin, 1979).
- [8] A. GRISEL, F. LÉVY, T. J. WIETING, Physica, 99B, 365 (1980) and A. GRISEL, PhD. Thesis, EPF, Lausanne, Switzerland, 1981.

- [9] R. LOUDON, Adv. Phys., 13, 423 (1964).
- [10] H. W. MYRON, B. N. HARMON and F. S. KHUMLO, J. Phys. Chem. Solids 42, 263 (1981).
- [11] Photoemission spectra of  $ZrS_3$  and  $Zr_{0.9}Ti_{0.1}S_3$  have been measured recently, which shows that the s and d orbitals of metals are mixed with the p orbitals of chalcogens in the valence band, especially under 4 eV below the Fermi level. More detailed results and discussion will be published in near future.
- [12] The detailed results will be published in near future.